Available online at www.sciencedirect.com
SCIENCE DIRECT®
ELSEVIER
Microelectronic Engineering 67–68 (2003) 865–871
MICROELECTRONIC ENGINEERING
www.elsevier.com/locate/mee

Rectangular channels for lab-on-a-chip applications

L. Ceriotti[a], K. Weible[b], N.F. de Rooij[a], E. Verpoorte[a,*]

[a] *SAMLAB, Institute of Microtechnology, University of Neuchâtel, Rue Jaquet-Droz 1, CH-2007 Neuchâtel, Switzerland*
[b] *Weible Optech, Rue Jaquet-Droz 7, CH-2007 Neuchâtel, Switzerland*

Received 19 September 2002; received in revised form 20 November 2002; accepted 14 January 2003

Abstract

We investigated the application of two technologies for the fabrication of rectangular microchannels with reasonable path lengths for UV detection in UV transparent materials. The first approach uses inductively coupled plasma (ICP)–reactive ion etching (RIE) to fabricate channels in fused silica wafers, using a 4-μm-thick nickel layer as protective mask. The effects of the process parameters on the etched channel profile and surface quality were studied directly using electron scanning microscopy, and indirectly through capillary electrophoresis experiments. In the second approach, narrow channels were easily realized in poly(dimethylsiloxane) (PDMS) using replica molding and dry-etched silicon masters. UV absorbance detection of tryptophan was possible vertically through these PDMS channels, using pre-aligned optical fibers to guide light to the channel and collect and bring the transmitted light to the detector.

Keywords: Fused silica; Poly(dimethylsiloxane); Rectangular channel; Reactive-ion etching

1. Introduction

The integration of UV absorbance detection for lab-on-a-chip applications (e.g. on-chip capillary electrophoresis (CE)) is not trivial. Since absorbance is proportional to the optical path length (Lambert–Beer law: $A = \varepsilon lc$, where A is the absorbance, ε the analyte's molar extinction coefficient, l the path length and c the analyte concentration), absorbance detection in microstructures could suffer from low sensitivity. To improve the optical path length in a microchannel, a U-shaped detector cell having a path length of 120–140 μm was integrated in a CE glass device for detection parallel to the flow [1]. An absorbance detection limit of 6 μM hydrolyzed fluorescein isothiocyanate dye at 488 nm was observed. Another approach to improve the optical path length was the fabrication of an optical

*Corresponding author. Tel.: +41-32-720-5442.
E-mail address: sabeth.verpoorte@unine.ch (E. Verpoorte).

0167-9317/03/$ – see front matter
doi:10.1016/S0167-9317(03)00148-5

cuvette right through the middle wafer of a three-layer glass chip. Also in this case, visible detection was performed in the direction of the flow [2]. Detection carried out vertically through the chip, perpendicular to the flow, generally yields insufficient sensitivity. This is because commonly used wet-etching techniques are isotropic, so that the resulting channels are twice as wide as they are deep. Channels with depths approaching reasonable optical path lengths would have volumes which would be too large for optimum separation performance. To enhance absorbance sensitivity in the visible range through these rounded glass channels, the effective optical pathlength was increased by integrating metal mirrors above and below the channel. In this way, the light is bounced back and forth through the cell several times [3].

To integrate UV absorbance effectively into a microfluidic system, the device has to include quartz windows or other UV-transparent materials, because glass absorbs light below 300–350 nm. To allow UV detection through isotropically etched quartz channels, an optical slit was integrated at the bonding interface of two quartz substrates, in order to effectively cut off the stray light [4]. Jackman et al. [5] proved the feasibility of performing on-line UV detection through a 60-μm-deep microchannel having SU-8 sidewalls and quartz windows at the top and bottom.

Since our goal was to achieve small detection volumes in a simple chip layout for CE separations, we decided to perform absorbance vertically through narrow microchannels. Two different ways to fabricate UV-transparent, rectangular microchannel structures were investigated. One approach consisted of the fabrication of 50-μm-deep quartz channels using inductively coupled plasma (ICP)–reactive ion etching (RIE) [6]. New results and a discussion of this fabrication method are presented in this paper. In the second approach, the channels were fabricated in poly(dimethylsiloxane) (PDMS) using replica molding with dry-etched silicon masters. The flexibility in PDMS channel geometry offered by the replication approach and its good transparency above 240 nm make this plastic an attractive substrate for UV absorbance applications. After sealing on a quartz chip, these hybrid PDMS/quartz chips were integrated in an optical system with pre-aligned optical fibers. Dye and amino acid samples were electrokinetically injected into the separation channel and detected by UV absorbance.

2. Experimental

2.1. Chip layout and sample injection

The channel layout used for both types of hybrid devices was designed for microchip CE, and had a 5-cm-long separation channel. Two offset 1-cm-long side channels intersected the separation channel to form a 200-μm-long double-T junction [7] (Fig. 1A). This intersection could be loaded with sample to form a 500-pl plug, which was then injected into the separation channel and driven towards the detection point by applying a high voltage along the separation channel. During the CE separation, push-back voltages were applied at the side channels to induce a small buffer flow to push sample back into the side channels, thus preventing sample leakage into the separation channel.

2.2. Fused-silica chip fabrication process

Fused-silica (quartz) wafers (100×0.525 mm) were purchased from Guinchard, Yverdon-les-Bains, Switzerland. The process for the fabrication of quartz structures by ICP–RIE was performed as

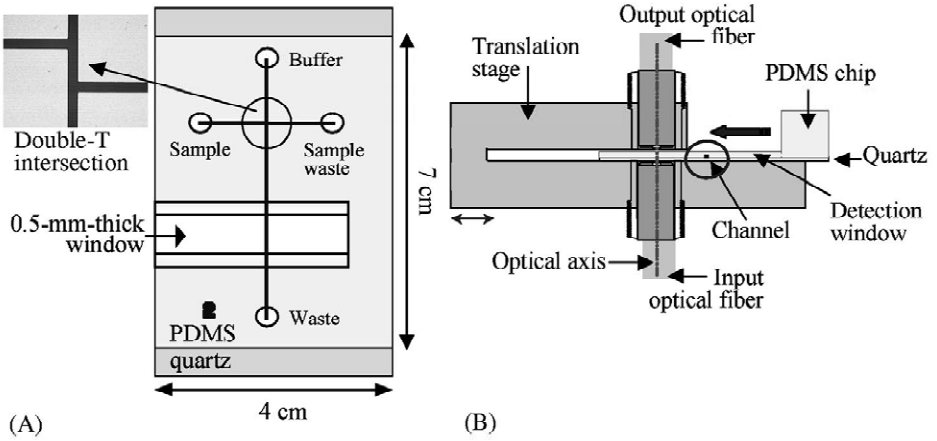

Fig. 1. (A) Top view of the PDMS chip containing channels for CE separations and a thin PDMS window for absorbance detection. The double-T intersection is presented in the insert on the left. (B) Cross-sectional view of the chip alignment with respect to the optical axis. The thin detection window is inserted between the two pre-aligned optical fibers.

follows. (1) Thin films of titanium (200 Å) and copper (3000 Å) are deposited consecutively on a clean quartz wafer by evaporation. (2) A positive photoresist optimized for thick layers (AZ 4562) is spin-coated onto the copper layer, and the channel structure is patterned by photolithography to obtain 8-μm-thick photoresist features. (3) Four μm of nickel is electroplated onto the exposed parts of the titanium/copper film around the patterned photoresist, using a commercially available bath (Nickel Sulfamate, Lea Ronal, Littau, Switzerland). (4) After photoresist stripping in acetone, the channels are selectively opened by first etching the copper with sodium persulfate (20 mg of $Na_2S_2O_8$ in 100 mg of deionized water), followed by removal of the titanium using buffered HF (BHF). (5) Finally, RIE is carried out with C_3F_8 as the gaseous etching agent in a Surface Technology Systems (STS) ICP–RIE system. The etch rate is 190 nm/min, a value which is lower than the etch rate reported for other optimized ICP–RIE systems (1 μm/min) [8]. (6) After fused silica etching, the nickel mask is removed using Aqua Regia (37% HCl–69% HNO_3, 3:1, v/v). The channels were sealed with a PDMS slab to circumvent the difficult quartz-to-quartz fusion bonding step, and used for CE tests.

2.3. PDMS chip fabrication

Masters for PDMS replicas were fabricated in silicon by deep reactive-ion etching (DRIE) as reported in [9]. Briefly, AZ 1518 positive photoresist is spin-coated onto a silicon wafer and patterned by photolithography. The wafer is then processed by DRIE in an STS machine. During the DRIE, the etchant species are directed perpendicularly at the wafer surface so that the areas surrounding the patterned photoresist channels are etched anisotropically. Smooth vertical structures of 50- and 70-μm height were obtained.

The Si master was fixed into a rectangular mold, and the PDMS pre-polymer/curing agent mixture (Sylgard 184, Dow Corning, Midland, MI, USA) cast onto it. This mold allowed the incorporation of a thin detection window (~ 0.5 mm) into the PDMS replica (Fig. 1). The polymerisation was performed at 65 °C for 4 h, after which the PDMS layer was peeled off the master. The structured PDMS device was then sealed on a 500-μm-thick quartz wafer cut to size.

2.4. Optical detection system

The PDMS chip was placed on the chip holder with the optical window inserted between two pre-aligned optical fibers (Ocean Optics, supplied by GMP, Renens, Switzerland) (Fig. 1B). The system was presented in Ref. [10] for a first series of tests. The input optical fiber (100 μm core diameter) is used to guide UV light from the light source, a deuterium-halogen lamp (Ocean Optics), to the channel. The output optical fiber (200 μm core diameter) is used to collect the light that is transmitted by the sample for detection. The detector contains a bandpass filter (240–400 nm for UV and 632 nm for visible detection) (Edmund Industrial Optics), a photodiode (Burr-Brown Corporation), an amplifier and a low-pass electronic filter. The signal is analyzed by LabView (National Instruments, Austin, TX, USA).

3. Results and discussion

3.1. Fused-silica channels etched by ICP–RIE

Reactive-ion etching can be employed to fabricate high-aspect-ratio structures in quartz. Different parameters influence the RIE process, such as chamber pressure, applied voltage, gas composition and plasma density. Process optimisation is therefore empirical and time-consuming. For our process, we used C_3F_8 as gas, a coil power of 750 W and a nickel etch mask. The coil power used ensured a sufficient plasma density for the etch process. The impact energy of the ions is given by the chamber pressure and electrode plate power. During the plasma process, no feedback control of the ion energy was applied. The chamber pressure was kept low (between 2.5 and 5 mTorr) to give good directionality and to avoid ion energy loss due to ion collision. The use of the nickel mask and low electrode plate power increased the selectivity of the etch process to about 1:40 (nickel:quartz), compared with the 1:1 reported for a photoresist mask [11]. ESEM photos of quartz channels achieved using the process described above are presented in Fig. 2. In Fig. 2A, the significant channel roughness can be attributed to the low power applied to the electrode plate, a condition that was chosen to preserve the integrity of the nickel mask. As a result, the physical ion impact necessary to

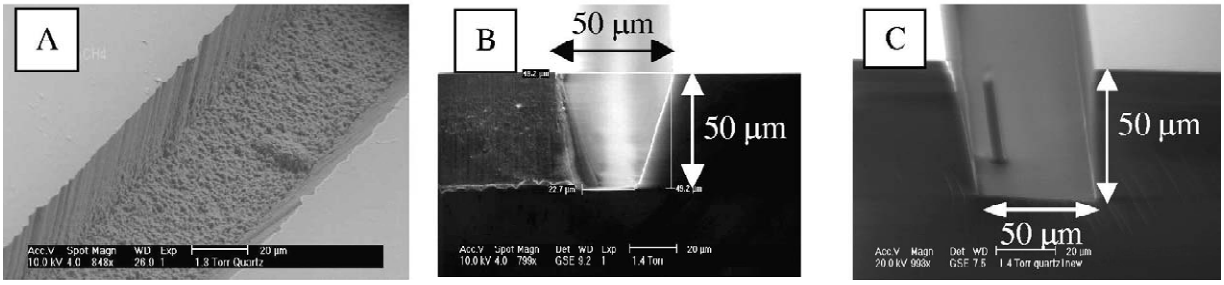

Fig. 2. ESEM photos of quartz channels (XL 30, ESEM-FEG, Philips). ICP–RIE process conditions: (A) Coil: 750 W, plate electrode: 50 W chamber pressure: 5 mTorr, 20 °C, C_3F_8 gas with CH_4. (B) Coil: 750 W, plate electrode: 120 W, chamber pressure: 2.5 mTorr, 20 °C, C_3F_8 gas only. (C) Coil: 750 W, plate electrode: 180 W, chamber pressure: 3.5 mTorr, 20 °C, C_3F_8 gas only.

break Si bonds was not enough, and the etching was not effective. Surface roughness, as well as geometric features in the column, could interfere with CE separation performance by modifying the EOF and producing a strong broadening effect, as reported for powder-blasted channels [12]. In these devices, the roughness is in the order of 8–10 μm and peak broadening is evident. Surface roughness in the order of a few nm, as is usually the case for wet-etched microchannels, does not have any observable effect on the separation performance [13]. By increasing the electrode plate power, a 50×50 μm channel was fabricated. Though smooth walls were obtained, wall verticality was not very good (Fig. 2B). Besides limiting the aspect-ratio of the channels achievable by this dry etch process, the non-verticality of the sidewalls could cause light scattering. Another etched structure obtained at higher electrode plate power and chamber pressure is presented in Fig. 2C. In this case, the verticality of the walls and the smooth surfaces look promising. The apparent non-verticality of the left channel wall is an optical effect. Some needle-like structures like that in Fig. 2C were observed, however. These could be due to deposition of fluorocarbon (CF_x) particles in the channel, which would act as a micromask during the etching process [14]. A CF_x film is also deposited on the structures during the RIE process [15]. This coating could be responsible for the low electroomotic flow found when performing CE experiments in the quartz/PDMS chips (laser-induced fluorescence detection was used in these tests [9]). The formation of the CF_x polymer in the plasma could be reduced by increasing the fluorine-to-carbon ratio (F/C), for example, by adding CF_4 to the C_3F_8 gas, as reported by Oki et al. [16]. This option was unfortunately not available in our RIE system.

3.2. Absorbance through PDMS/fused-silica chips

To test the performance of the absorbance detection system in the UV and visible range, different concentrations of methylene blue (MB) ($\varepsilon_{632\ nm}=42\ 960\ cm^{-1}\,M^{-1}$) were injected into the PDMS channel. A limit of detection (LOD) of 1 μM MB was found at 632 nm. In the UV, an LOD of 5 μM MB was found, due to the different light source and band pass filter used, and the reduced photodiode response in the UV range. The detection system was also employed to detect 0.1 mg/ml (0.5 mM) of the aromatic amino acid, tryptophan ($\varepsilon_{279\ nm}=5574\ cm^{-1}\,M^{-1}$). The tryptophan peak is presented in Fig. 3. An LOD of 0.03 mg/ml (0.15 mM) is estimated for this analyte. Note that the absorbance signal grows, as expected, when channel depth increases from 50 to 70 μm. The peaks are relatively broad, due mainly to manual switching between the injection and separation modes. The peak signal is also smaller than expected on the basis of Lambert–Beer law. This can partly be explained by the fact that the band-pass filter is centred at 310 nm, while the $\lambda_{max\ abs}$ for tryptophan is 279 nm. The wide spectral bandwidth used may also contribute to lower peak intensity.

4. Conclusions

Two approaches were investigated to fabricate rectangular microchannels for UV detection perpendicular to the flow. In the first approach, channels were etched in quartz using dry etching. The development of this process, which is sensitive to many parameters, needs optimization. In particular, the formation of the fluorocarbon polymer during etching should be prevented to get smooth and reproducible surfaces, which are necessary for lab-on-a-chip applications. Moreover, the fabrication of

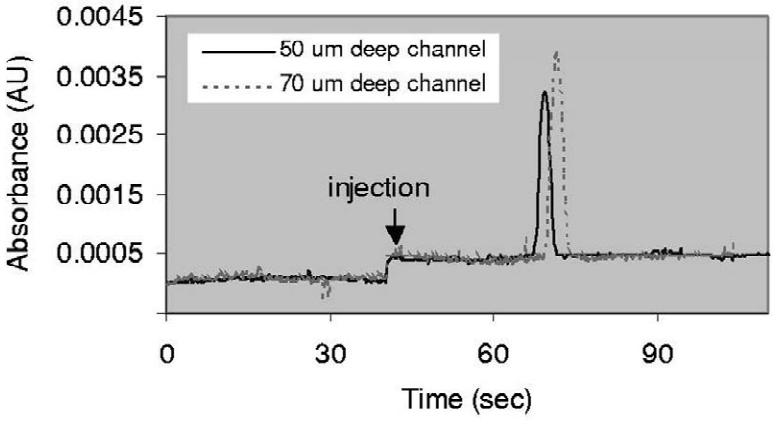

Fig. 3. UV absorbance peak of 0.1 mg/ml tryptophan through 50- and 70-μm deep channels in different PDMS/quartz chips. Running buffer: 20 mM Tris–HCl, pH 7.6; E_{sep}: 400 V/cm; L_{eff}: 2.5 cm. The different migration times of the peaks are due to manual switching between injection and separation modes.

a wholly quartz channel should improve system performance with respect to the hybrid quartz-PDMS channel used in this study, since quartz possesses better UV transmission properties than PDMS. In the second approach, rectangular channels were easily realized in PDMS by replica molding of a master fabricated in silicon by DRIE. UV absorbance detection of tryptophan plugs was possible through these channels because of the good optical properties of this polymer. Modification of the optical and electronic components of the detection system should improve system performance and allow detection of other biological species, such as peptides and DNA fragments.

Acknowledgements

The authors thank the service of Microscopy and Nanoscopy of IMT for the ESEM photos. Professor R. Dändliker and S. Clément (Applied Optics group, IMT, Neuchâtel) are also acknowledged for the realization of the optical system. Thanks go also to SAMLAB group members, Dr S. Koster for his help in preparation of this manuscript, and J. Lichtenberg for assistance in building detection electronics. This work was financially supported by the Swiss Commission for Technology and Innovation Program MedTech.

References

[1] Z. Liang, N.H. Chiem, G. Ocvirk, T. Tang, K. Fluri, D.J. Harrison, Anal. Chem. 68 (1996) 1040.
[2] A. Daridon, V. Fascio, J. Lichtenberg, R. Wütrich, H. Langen, E. Verpoorte, N.F. de Rooij, Fresenius J. Anal. Chem. 371 (2001) 261.
[3] H. Salimi-Moosavi, Y.T. Jiang, L. Lester, G. McKinnon, D.J. Harrison, Electrophoresis 21 (2000) 1291.
[4] H. Nakanishi, T. Nishimoto, A. Arai, H. Abe, M. Kanai, Y. Fujiyama, T. Yoshida, Electrophoresis 22 (2001) 230.
[5] R.J. Jackman, T.M. Floyd, R. Ghodssi, M.A. Schmidt, K.F. Jensen, J. Micromech. Microeng. 11 (2001) 263.

[6] L. Ceriotti, E. Verpoorte, K.J. Weible, N.F. de Rooij, in: Proceedings of Transducers '01, Munich, Germany, 2001, p. 1174.
[7] C.S. Effenhauser, A. Manz, H.M. Widmer, Anal. Chem. 65 (1993) 2637.
[8] X.D. Li, T. Abe, M. Esashi, Sensors Actuators A 87 (2001) 139.
[9] L. Ceriotti, N.F. de Rooij, E. Verpoorte, Anal. Chem. 74 (2002) 639.
[10] L. Ceriotti, J. Lichtenberg, S. Clément, P. Nussbaum, E. Verpoorte, R. Dändliker, N.F. de Rooij, in: Proceedings of Micro Total Analysis Systems 2001, Monterey, CA, USA, 2001, p. 339.
[11] P. Nussbaum, K.J. Weible, M. Rossi, H.P. Herzig, in: Proceedings of SPIE Conference on Micromachine Technology for Diffractive and Holographic Optics, Santa Clara, CA, USA, 1999, p. 63.
[12] D. Solignac, A. Sayah, S. Constantin, R. Freitag, M.A.M. Gijs, Sensors Actuators A 92 (2001) 388.
[13] B.H. Weiller, L. Ceriotti, T. Shibata, D. Rein, M.A. Roberts, J. Lichtenberg, J.B. German, N.F. de Rooij, E. Verpoorte, Anal. Chem. 74 (2002) 1702.
[14] W.W. Stoffels, E. Stoffels, G.M.W. Kroesen, M. Haverlag, J.H.G. den Boer, F.J. de Hoog, Plasma Sources Sci. Technol. 3 (1994) 320.
[15] M. Haverlag, E. Stoffels, W.W. Stoffels, G.M.W. Kroesen, F.J. de Hoog, J. Vac. Sci. Technol. A 12 (1994) 3102.
[16] A. Oki, S. Adachi, Y. Takamura, K. Ishiara, H. Ogawa, Y. Ito, T. Ichiki, Y. Horiike, Electrophoresis 22 (2001) 341.